Anal Bioanal Chem (2013) 405:51–61
DOI 10.1007/s00216-012-6422-8

REVIEW

Towards analytically useful two-dimensional Fourier transform ion cyclotron resonance mass spectrometry

Maria A. van Agthoven · Marc-André Delsuc · Geoffrey Bodenhausen · Christian Rolando

Received: 23 September 2011 / Revised: 6 August 2012 / Accepted: 12 September 2012 / Published online: 18 October 2012

Abstract Fourier transform ion cyclotron resonance (FT-ICR) mass spectrometry (MS) achieves high resolution and mass accuracy, allowing the identification of the raw chemical formulae of ions in complex samples. Using ion isolation and fragmentation (MS/MS), we can obtain more structural information, but MS/MS is time- and sample-consuming because each ion must be isolated before fragmentation. In 1987, Pfändler et al. proposed an experiment for 2D FT-ICR MS in order to fragment ions without isolating them and to visualize the fragmentations of complex samples in a single 2D mass spectrum, like 2D NMR spectroscopy. Because of limitations of electronics and computers, few studies have been conducted with this technique. The improvement of modern computers and the use of digital electronics for FT-ICR hardware now make it possible to acquire 2D mass spectra over a broad mass range. The original experiments used in-cell collision-induced dissociation, which caused a loss of resolution. Gas-free fragmentation modes such as infrared multiphoton dissociation and electron capture dissociation allow one to measure high-resolution 2D mass spectra. Consequently, there is renewed interest to develop 2D FT-ICR MS into an efficient analytical method. Improvements introduced in 2D NMR spectroscopy can also be transposed to 2D FT-ICR MS. We describe the history of 2D FT-ICR MS, introduce recent improvements, and present analytical applications to map the fragmentation of peptides. Finally, we provide a glossary which defines a few keywords for the 2D FT-ICR MS field.

Keywords Mass spectrometry · Fourier transform ion cyclotron resonance · Two-dimensional · FT-ICR

M. A. van Agthoven · C. Rolando (✉)
Miniaturisation pour la Synthèse l'Analyse et la Protéomique, USR CNRS 3290, Institut Michel-Eugène Chevreul, FR CNRS 2638 and Protéomique, Modifications Post-Traductionnelles et Glycobiologie, IFR 147 Université de Lille 1, Sciences et Technologie,
59655 Villeneuve d'Ascq Cedex, France
e-mail: Christian.Rolando@univ-lille1.fr

M.-A. Delsuc
U 596 and UMR CNRS 7104, Institut de Génétique et de Biologie Moléculaire et Cellulaire, INSERM, Université de Strasbourg,
1 rue Laurent Fries,
67404 Illkirch-Graffenstaden, France

G. Bodenhausen
UMR 7203, Département de Chimie, École Normale Supérieure,
24 rue Lhomond,
75231 Paris Cedex 05, France

Introduction

Fourier transform ion cyclotron resonance (FT-ICR) mass spectrometry (MS) was developed in 1973 by Comisarow and Marshall [1] as a method to measure the cyclotron motion of ions in a high magnetic field, calculate their frequencies, and convert this information into mass spectra. Ever since its inception, this technique has provided the highest resolving power and mass accuracy in mass analysis, and has grown into a powerful tool for the analysis of complex mixtures. To maximize the versatility of FT-ICR MS for a broad range of samples, it has been coupled with almost all ion sources: electron impact, chemical impact, fast atom bombardment, electrospray ionization (ESI), matrix-assisted laser desorption ionization, atmospheric pressure photoionization [2], and recently metastable atom bombardment [3].

Transfer optics have been developed and optimized to allow differential pumping between sources at atmospheric pressure and the ultra-high-vacuum cell for ion cyclotron resonance (ICR) to accumulate ions externally and thus improve sensitivity [4, 5]. To gain more structural information, many fragmentation modes have also been implemented in FT-ICR MS, from classic collision-induced

dissociation (CID) to infrared multiphoton dissociation (IRMPD), electron capture dissociation (ECD), sustained off-resonance irradiation, electron transfer dissociation (ETD), or blackbody infrared radiative dissociation [6]. In MS/MS, ions are isolated, either before trapping in the ICR cell or inside the ICR cell, and are then fragmented in order to obtain detailed information on the molecular structure of the ions.

The commonest configuration of the interface between the ion source and the FT-ICR cell is composed of a cell for ion accumulation, a quadrupole analyzer or a linear ion trap for ion selection, and a cell for ion dissociation. This configuration has several advantages: (1) the ion accumulation cell increases sensitivity by trapping ions during the ICR duty cycle, thus increasing the number of ions that can be injected into the ICR cell; (2) collision cells can be fitted for both CID and ETD [7]; (3) the linear ion trap allows one to perform several MS/MS analyses at low resolution during high-resolution acquisition by FT-ICR of the precursor ions [8]. External isolation and fragmentation is easily automated, and is often used for liquid chromatography (LC)–MS/MS in proteomics [9]. Because they induce cleavages at different bonds, external CID and ETD used in combination allow one to achieve the sequencing of peptides and the identification and localization of posttranslational modifications [10].

FT-ICR MS is based on the cyclotron motion of charged particles in a homogeneous magnetic field: ions move in circular trajectories that are orthogonal to the magnetic field with a frequency that is proportional to the intensity of the field and inversely proportional to their mass-to-charge (m/z) ratio. When the ions are close to a detection plate of the ICR cell, Coulomb interactions with the conduction electrons in the metal induce an image current. This current can be amplified and converted to a digital signal that is sampled at regularly spaced intervals (the data set thus measured is called the time transient). The frequencies contained in this signal can be separated by Fourier transformation and converted into a mass spectrum.

Cyclotron frequencies are proportional to magnetic field strength:

$$f = \frac{qB}{2\pi m}, \tag{1}$$

where f is the cyclotron frequency, m the mass of the ion, q the electric charge of the ion, and B the magnetic field strength. Since FT-ICR MS is a temporal measurement, sensitivity and resolution largely depend on how long the signal can be measured. On a physical level, this means the coherence of ion packets must be maintained as long as possible. The two factors that most influence how long an ion packet remains coherent are the pressure in the ICR cell [11] and the geometry of its electrodes [12]. Guan et al. [11] showed that the ion–neutral collision mechanism closely follows the hard-sphere model, in which the intrinsic full width at half maximum of a peak in the frequency domain can be expressed as

$$\Delta f_{50\%}^{Intrinsic} = \frac{1}{\pi\tau}, \tag{2}$$

where τ is the lifetime of the ion packet, which depends on pressure, ion collisional cross section, magnetic field, trapping potentials, and cell geometry. At high pressure or for long acquisition times (i.e., $T \gg \tau$, where T is the acquisition time), mass resolving power is proportional to the magnetic field strength and is limited by the lifetime of the ion packet:

$$\frac{m}{\Delta m_{50\%}} \propto \frac{qB\tau}{m}. \tag{3}$$

At low pressure or short acquisition times ($T \ll \tau$), $f_{50\%}^{Intrinsic}$ is much smaller than $\Delta f_{50\%}^{Observed}$, which is inversely proportional to the duration of detection [13]. As a result, for low pressure or a short acquisition time, mass resolving power is proportional to T [6]:

$$\frac{m}{\Delta m_{50\%}} \propto \frac{qBT}{m} \tag{4}$$

In most cases, T is the limiting factor for the mass resolving power, but for very long acquisition times or super-resolution measurements [14], τ gives the maximum resolving power of the instrument.

The time transient is regularly sampled. Because of the Shannon–Nyquist theorem, the sampling frequency has to be twice the highest frequency present in the signal, i.e., the frequency of the lowest m/z ratio. The acquisition time T can be expressed as

$$T = 2N \times f_N, \tag{5}$$

where N is the number of data points and f_N is the Nyquist frequency. On most instruments the parameters that are set by the user are the lower mass observed, which determines the Nyquist frequency, and the number of data points stored in the computer memory. So the working resolving power is inversely proportional to the starting mass, and is proportional to the number of data points. A typical time transient is measured over 524,288 data points (in general, powers of 2 are favored, because this makes Fourier transform calculations faster). Starting at m/z 86 leads to a time transient lasting several hundred milliseconds in the commonest magnetic fields (7 or 9.4 T). The highest magnetic field currently available for FT-ICR MS is 15 T. This leads to resolving powers that can easily exceed 10^6, with mass accuracies that are routinely well below 1 ppm after proper calibration. In complex mixtures with several tens of thousands of compounds, we can therefore identify the elemental composition

of ions up to approximately 1,000 Da. Ions with mass differences smaller than the mass of one electron (0.000549 Da) have been separated with *m*/*z* 453.2496 and *m*/*z* 453.2499 [15]. The baseline isotopic pattern resolution of bovine serum albumin (*m*=66 kDa, *z*=63) [16] and unit mass baseline resolution for a 148-kDa monoclonal antibody have recently been achieved [17].

When ions with analytically useful *m*/*z* ratios (*m*/*z* 10–10,000) are injected in the ICR cell, their cyclotron radius is less than 1 mm, so the ions are too far away from the detection plates to induce a detectable signal. To increase sensitivity, the ions must be excited by a resonant radio-frequency (RF) voltage. This brings coherent packets of ions into orbits with larger radii, thus improving sensitivity. The basic electrodes necessary for an ICR cell therefore comprise two excitation plates to apply excitation RF pulses to bring the ions into orbits with large radii, two detection plates to measure the image current, and two trapping plates to trap the ions axially with an electric potential well (radial trapping being ensured by the magnetic field). The commonest ICR cell geometry is the Infinity cell [18]: the four excitation and detection plates form a cylinder that is cut into four slices (the symmetry axis of the cylinder being parallel to the magnetic field), and the cylinder is closed by trapping plates. This ICR cell was used, among others, for the analysis of bovine serum albumin mentioned earlier. The compensated ICR cell introduced by Gabrielse et al. [19] for high-accuracy isotope mass measurement has been extended to analytical FT-ICR by Tolmachev et al. [20] and Brustkern et al. [21], who showed that it eliminates harmonics in the signal [16]. An asymmetric variation on this geometry in which the excitation and detection plates do not have the same geometry was developed by Kaiser et al. [22] for complex mixtures. The harmonized ICR cell recently introduced by Nikolaev et al. [23, 24] enables the recording of very long time transients up to 3 min and achieved an ultrahigh resolution of 2.4×10^7 for reserpine.

For ions to be excited in a resonant fashion, the frequency of the RF excitation needs to match their cyclotron frequency. The radial component of the electric interaction between the ions and the excitation field is then centrifugal and the radius of the ion packets increases. Ions with the same *m*/*z* ratio and therefore the same cyclotron frequency are excited coherently in packets: their motion is in phase with the excitation voltage. Up to a certain radius, ion cyclotron radii are proportional to the RF amplitude and the duration of the excitation [25]. Most FT-ICR mass analyzers use frequency-swept ("chirp") excitation [26], but an alternative technique called stored-waveform inverse Fourier transform (SWIFT) uses an inverse Fourier transform of a rectangular excitation frequency spectrum to obtain a waveform that is applied to the excitation plates [27]. During excitation, ionic radii are not affected by off-resonance RF voltages [28, 29] because the pulses in the microsecond to tenths of microsecond range are too short to cause even a single off-resonance acceleration–deceleration cycle or even increase the kinetic energy in a significant way. The sustained off-resonance irradiation dissociation technique requires an irradiation time of hundredths of a microsecond to milliseconds [30].

Ion de-excitation and the emergence of 2D FT-ICR MS

In 1984, Marshall et al. [31] showed that it is also possible to de-excite ions in an ICR cell after they have been resonantly excited. In one experiment, they excited ions with resonant pulses of increasing duration and measured the relative ICR signal magnitude. In a second experiment, they inverted the phase of the excitation voltage after 1.0 ms. Figure 1 shows the relative ICR signal magnitude measured in both experiments as a function of the duration of the excitation pulse. For ions that are excited with a constant phase, the relative ICR signal magnitude increases with the cyclotron radius until the ions are defocused or reach the electrodes of the ICR cell. However, the phase inversion causes the ionic radius and hence the relative ICR signal magnitude to decrease. The sign of the potential on the excitation plates has changed, and the ions, instead of being attracted by the excitation plate they are closest to, are repelled by it: the electric force has become centripetal instead of centrifugal. This observation proved that the

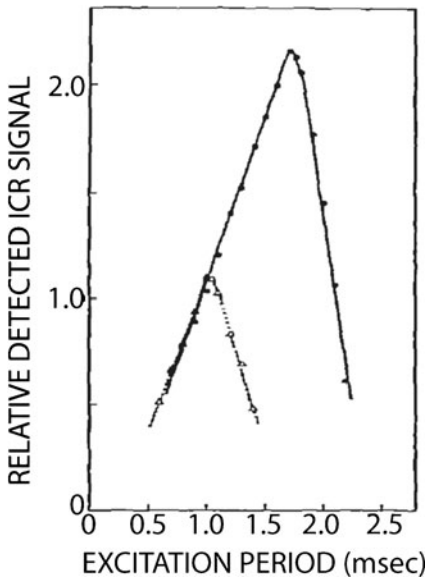

Fig. 1 Ion cyclotron resonance (*ICR*) signals of $C_9F_{20}N^+$ from perfluorotributylamine (*m*/*z* 501.971) after resonant excitation with a pulse with constant phase of increasing length (*filled circles*) and after resonant excitation where the phase is shifted through 180° after 1.0 ms (*open triangles*). (Reproduced with permission from Marshall et al. [31])

excitation of ions is highly linear and additive in an ICR cell, so the "'de-excitation" of ions is possible in an ICR cell as long as they stay coherent.

This discovery came hand in hand with the development of phase-shifted swept-frequency or notch ejection, first by Noest and Kort [32] and later by Vulpius and Houriet [33]. The frequency spectrum of the RF excitation pulse features a triangular dent or "notch" at the cyclotron frequency of the ion species to be isolated, which can be achieved by introducing a phase inversion when the pulse reaches this frequency. This technique can excite and eject ions of all m/z ratios (or cyclotron frequencies) in the ICR cell except for one chosen m/z ratio. Noest and Kort [32] showed that the breadth of the mass window is inversely proportional to the m/z ratio of the selected ions and inversely proportional to the square root of the sweep rate. Vulpius and Houriet [33] showed that notch ejection is efficient and clean regardless of the relative abundance of the selected ion species and of the remaining ion species that are to be ejected.

The reversibility of ion excitation in an ICR cell has been exploited in the very low energy CID (VLE-CID) method developed by Boering et al. [34]. In this experiment, molecular radical cations of *n*-butylbenzene were successively accelerated and decelerated by resonant excitation in which the phase was inverted periodically in the presence of argon. As a result, the cyclotron radius of the ions increased and decreased periodically and the average kinetic energy of the ions was lower than in the usual in-cell CID experiments [35], in which ions are excited to a large radius before the gas is injected into the ICR cell. In VLE-CID, ion–molecule collisions occur at lower energies than in the usual in-cell CID, and the lowest-energy fragmentation pathways are favored. However, in notch ejection and VLE-CID, only one ion species is de-excited, and the difference between the phase of the RF pulse and the phase of the ion packet is either 0° or 180°.

Here it is of interest to discuss the nature of the phase difference between the RF pulse and the ion motion. The phase of the RF pulse is $\theta=\omega t+\varphi$ if the RF voltage is described by

$$V_{RF}(t) = V_0 \cos(\omega t + \varphi), \tag{6}$$

where V_0 is the amplitude of the oscillation, ω its frequency (which is time-dependent), and φ the initial phase at $t=0$. For an isolated ion (or, equivalently, for a packet of ions), the phase corresponds to one of the cylindrical coordinates of the ion's location in a plane orthogonal to the magnetic field:

$$\theta = \omega t + \phi, \tag{7}$$

where ω is the ion's cyclotron frequency and ϕ the arbitrary initial phase at $t=0$ (in our approximation, we do not make a distinction between a single ion and a coherent ion packet). In the steady state (i.e., when $t \gg 2\pi/\omega$), the interaction between the ions and the off-resonance RF voltage is negligible, owing to the short duration of the excitation pulse, so we are only interested in the interaction between the ions and resonant RF voltages that match the cyclotron frequency. Hence, the phase difference between the RF pulse and the ion packet is φ - ϕ, which can be arbitrarily defined as 0° when the ions are at the center of one arbitrary excitation plate when the RF voltage has reached its positive maximum, and 180° when the ions are at the center of the opposite excitation plate when the RF voltage is at its negative minimum.

In 1987, a joint effort by Bodenhausen's NMR group at the University of Lausanne and Gäumann's FT-ICR MS group at the Ecole Polytechnique Fédérale de Lausanne in Switzerland led to a 2D FT-ICR MS experiment [36–38]. This experiment is analogous to nuclear Overhauser effect spectroscopy or exchange spectroscopy in the NMR field [39] and is reminiscent of selective de-excitation of ions in an ICR cell. The pulse sequence of this experiment is shown in Fig. 2, as is the dependence on the evolution interval t_1 of the relative ICR signal magnitude of CH_3^+, $CH_4^{\bullet+}$, and CH_5^+ ions in this experiment.

After ionization near the center of the ICR cell, two RF pulses are applied to the excitation plates, separated by an evolution interval or frequency encoding period t_1. The first pulse excites the ions coherently to a large cyclotron radius and is called the excitation pulse. Ions are then left to rotate in packets during t_1. A second identical RF pulse does not have the same effect as the first one, since the ions at the beginning of the second pulse have a large radius and their relative phase with regard to the second pulse is proportional to the product of their cyclotron frequency and t_1 (this pulse is called the encoding pulse). This relationship is identical for monochromatic pulses and for frequency-swept pulses. The cyclotron radius of the ions at the end of the second pulse also depends periodically on both the cyclotron frequency and the delay t_1.

At the end of the second pulse, the ions are therefore distributed over different cyclotron radii depending on their cyclotron frequencies. In the initial 2D FT-ICR MS experiments, the ions produced by electron ionization of methane and excited at different cyclotron radii by the first two pulses were allowed to collide during a mixing interval τ_m with methane, which was injected into the ICR cell. For an energy distribution corresponding to a temperature above room temperature, the efficiency of most ion–molecule reactions decreases with the collision energy, i.e., with the kinetic energy of the colliding ions, which increases with their cyclotron radius. Therefore, the abundance of the fragment ions has a periodic dependence on the cyclotron radius of the precursor ions and hence on t_1.

After reaction or metastable dissociation, all ions are re-excited using a third resonant excitation pulse (or observe pulse) in order to detect both precursor and fragment ions. The relative ICR signal magnitude of the precursor ions is proportional to

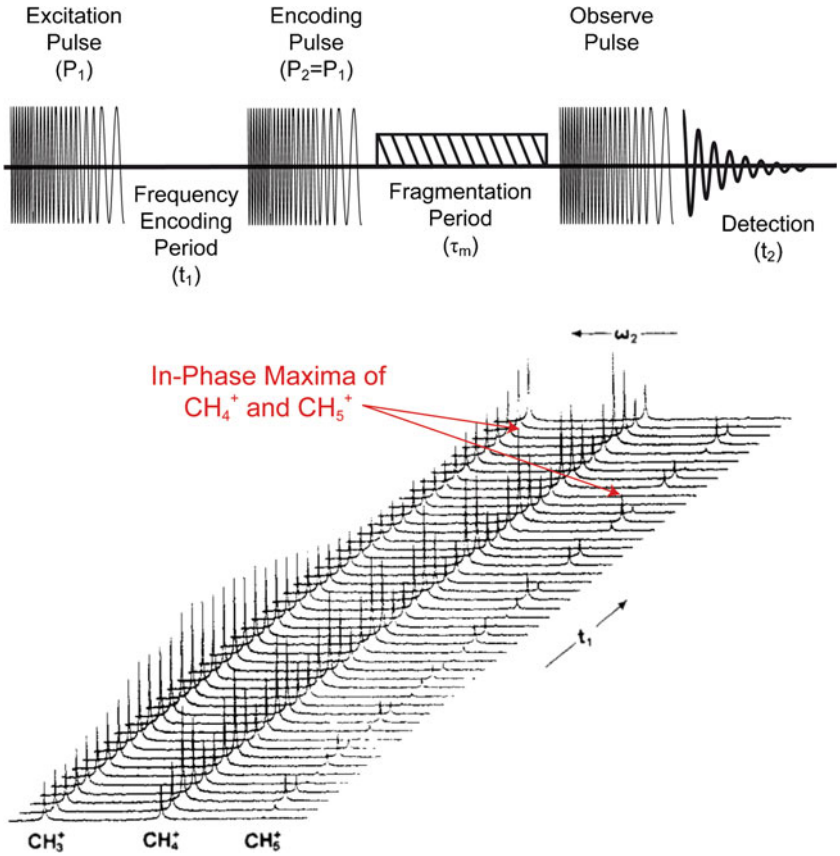

Fig. 2 Pulse sequence of 2D Fourier transform ICR (FT-ICR) mass spectrometry (MS) proposed by Pfändler et al. (*top*) and evolution of the product ion peaks induced by ionizing methane by electron ionization with the evolution interval t_1 between the first two radiofrequency pulses (*bottom*). *ECD* electron capture dissociation, *IRMPD* infrared multiphoton dissociation. (Adapted with permission from Pfaendler et al. [37])

both their cyclotron radius (i.e., to the product of their cyclotron frequency and t_1) and their abundance. The relative ICR signal magnitude of the product ions is proportional to their abundance, i.e., to the radius of their precursors, which is determined by the product of the cyclotron frequency of these precursors and t_1.

CH_5^+ is a product ion which is created by ion–molecule reactions between $CH_4^{\bullet+}$ and neutral methane [40]. The frequency of the relative ICR signal magnitude of CH_5^+ in the t_1 interval is therefore equal to the cyclotron frequency of its $CH_4^{\bullet+}$ precursor. This is evident in Fig. 2, where the CH_5^+ peak is maximum when the $CH_4^{\bullet+}$ peak is also maximum. CH_3^+ is both a precursor that is present at the start of the pulse sequence and a product of collisions involving $CH_4^{\bullet+}$. Its ICR signal therefore has two frequencies in the t_1 interval: its own cyclotron frequency and the cyclotron frequency of $CH_4^{\bullet+}$.

By recording FT-ICR mass spectra using systematically incremented durations $t_1 = n_1 \times \Delta t_1$ (in which n_1 is the number of increments, with n_1^{max} giving the resolution in the vertical dimension, and Δt_1 the increment, which gives us the sampling rate and the Nyquist frequency, i.e., the lowest m/z ratio in the vertical dimension), one can observe the modulations of the relative ICR signal magnitude of all ions in a sample and correlate them with the relative ICR signal magnitudes of their fragments. It is sufficient to calculate the Fourier transform of each time transient recorded as a function of the detection interval t_2 and to calculate another Fourier transform as a function of the evolution interval t_1. In the resulting 2D cyclotron frequency spectrum, all fragment ion peaks appear along the ω_2 axis (usually plotted horizontally) and their precursors appear along the ω_1 axis (which is by convention plotted vertically).

This pulse sequence has the potential to offer an efficient alternative to FT-ICR MS/MS. Indeed, whereas in MS/MS the ions of interest must first be identified by the user before setting the isolation and fragmentation parameters, in 2D FT-ICR MS all ions in the sample can be fragmented at the same time. Furthermore, ion isolation can lead to ion losses and therefore to losses in sensitivity. In a 2D FT-ICR MS experiment, the ions need not be isolated in the ICR cell. Finally, because of the properties of the Fourier transform, all time transients that are acquired contribute to the signal-to-noise ratio of all ion species in the sample, both of precursor ions and of their fragments, whereas in MS/MS the time transients that are accumulated for each spectrum only serve to improve the signal-to-noise ratio of one selected parent ion and its fragments [41].

Pfändler et al. recognized that CID and ion–molecule reactions are not the only fragmentation modes that can be used for 2D FT-ICR MS: any process leading to new ions whose efficiency depends on the cyclotron radius of the precursor ions can be used. In a subsequent study, they

recorded a 2D FT-ICR mass spectrum using IRMPD as a fragmentation mode [38]. Because the laser beam is focused on the center of the ICR cell, only ions that have been de-excited towards the center of the cell can be fragmented. As a result, the abundance of fragment ions depends on t_1 and the cyclotron frequency of the precursor just like in the original experiment.

The main issue that limited the scope of the first 2D FT-ICR studies was the limited capacities of computers in terms of memory size and speed. The largest spectrum that was recorded in these experiments consisted of 512 time transients each comprising 8,192 data points [38]. To achieve high resolution and mass accuracy in broadband mode, the number of data points that need to be recorded per time transient is at least 64 times larger. This means that, for two decades, research in 2D FT-ICR MS was stalled by computer limitations.

In 1993, Ross et al. [42] developed an alternative to the original pulse sequence described by Pfändler et al. for 2D FT-ICR MS called stored-waveform ion radius modulation (SWIM). Whereas Pfändler et al. used two frequency sweeps to modulate the cyclotron radii of the ions, by using the high linearity of FT-ICR ionization, Ross et al. combined these two pulses into one pulse. Ross et al. created 512 distinct waveforms with a periodic variation of the RF amplitude, so the resulting ion radii had a similar periodicity. In this technique, the frequency of this variation is designed to increase linearly with cyclotron frequency. For each frequency spectrum, the inverse Fourier transform is calculated and the resulting RF voltage is applied to the excitation plates for N different waveforms before injecting the gas into the ICR cell, re-exciting the ions, and recording the time transient. Instead of calculating the Fourier transform as a function of the evolution interval t_1, one calculates it as a function of the waveform number n=1, 2… N.

In 2001, van der Rest and Marshall [43] used 2D SWIM CID FT-ICR MS to study proton-bound and sodium-bound heterodimers of amino acids. In 2002, Ross et al. [44] applied SWIM to products of combinatorial synthesis of pharmaceutical interest and to a sample of coating for car finishes. This was the first truly analytical study on complex samples using 2D FT-ICR MS.

Both van der Rest and Marshall and Ross et al. observed that the signal is plagued by a large amount of scintillation noise (as it is known in astronomy [45]), which is equivalent to t_1 noise (as it is known in NMR spectroscopy [46]). This leads to vertical streaks in 2D spectra at the ω_2 frequencies of the most intense peaks. Scintillation noise stems from fluctuations in the amplitude or frequency of a signal and cannot be reduced by accumulating several scans, as it is proportional to the signal. In astronomy, scintillation noise comes from atmospheric turbulence, which causes stars to twinkle, whereas in NMR spectroscopy t_1 noise is caused by various sources of instability. Contrary to NMR spectroscopy, which always uses the same set of nuclei after a recovery period during a given experiment, 2D FT-ICR MS uses a new bunch of ions for each time increment in the first dimension. So, in 2D FT-ICR MS, the most likely cause of scintillation noise is the fluctuation in the number of ions created in the ion source, which is why the astronomical terminology seems appropriate.

Other approaches to correlate several precursor ions and their fragments

Another approach that has been developed is Hadamard encoding of the excitation [47, 48]. Hadamard FT-ICR MS consists in applying a suitable comb to the frequency sweep and applying the appropriate Hadamard transform to the resulting mass spectra. Hadamard FT-ICR MS has the power to encode all ions in the MS spectrum by dividing the mass range into equal segments, but to the best of our knowledge it has been used only using a data-dependent encoding of the excitation matrix, leading to a sensitivity gain of $0.5 \times \sqrt{n}$, where n is the number of multiplexed peaks. Like 2D FT-ICR MS, Hadamard encoding is sensitive to scintillation noise, leading to negative peaks [49]. Two other approaches not using a mathematical formalism have been described. The first one is based on the a priori knowledge of the dissociation of the ion precursors as in the case of peptides and on high mass accuracy obtained in an FT-ICR experiment. The fragment ions from up to seven ions selected simultaneously using a SWIFT waveform may be associated with their precursors, leading to a multiplexed acquisition [5]. Precursor acquisition independent from ion count (PAcIFIC) is also data-independent and combines LC with MS/MS by repeating LC runs with constant mass selection and scanning the mass range for isolation [50]. PAcIFIC can be used with a variety of mass analyzers, but the number of runs required is proportional to the mass range and inversely proportional to the isolated mass range, so it is extremely time- and sample-consuming [51]. For example, in a typical proteomics analysis, for each LC run, ten mass spectra separated by an increment of m/z 1.5 using an m/z 2.5 isolation window are recorded with a relatively long acquisition time of 3.0 s per spectrum. To cover the m/z 400–1,400 mass range, 67 LC runs each covering 15 mass units are required, leading to a total acquisition run time of 4.2 days using a classic 90-min LC run time. Here also in the case of coelution the identification is based on known fragmentation. The main advantage of PAcIFIC is linked to the high dynamics allowed by the chromatographic separation before the multiplexed acquisition of the data. The recently introduced SWATH method is based on the same principle but avoids the multiple injections of the same sample, taking advantage of the high acquisition capability

of new double-quadrupole time-of-flight instruments during the elution time of a chromatographically windowed MS selection covering the full useful mass range [52].

Recent developments in 2D FT-ICR MS

Since 2000, considerable advances have been made in mainstream computer capacity: from 2003 onwards, personal computers have been equipped with 64-bit processors, file systems, and improved operating systems. This increased speed, accuracy, the size of data files (which increased from 1 GB to 4 PB), and the size of accessible memory. The storage capacities of hard drive disks improved dramatically (the terabyte limit was broken in 2007), which facilitates the recording of large data sets. The electronics of FT-ICR MS acquisition systems have been fully digitized, thereby making excitation pulses very stable and allowing easy changes of the experimental protocol.

In this context, revisiting 2D FT-ICR MS in order to turn it into a fully fledged, high-resolution analytical technique became possible. In addition to the advances in data acquisition and processing, gas-free fragmentation techniques such as IRMPD and ECD have become routinely available on commercial FT-ICR instruments [53]. Because no gas needs to be injected into the ICR cell, the ions do not undergo collisions with neutrals and ion packets remain coherent. The use of ECD or IRMPD therefore improves both the sensitivity and the resolution of MS/MS and 2D FT-ICR MS.

In 2010, we implemented Pfändler's experiment on a 9.4-T ApexQE FT-ICR instrument from Bruker Daltonics (Bremen, Germany) with a positive nanoESI ion source and IRMPD as a fragmentation method [54]. Because of the improvements in FT-ICR technology, we were able to record time transients over an analytically useful mass range (*m*/*z* 87.67-2,000) in the (horizontal) ω_2 domain. The increment of the evolution time was Δt_1=0.3 μs, which corresponds to a maximum measured frequency of 1.667 MHz and an *m*/*z* 87.67-2,000 mass range in the (vertical) ω_1 domain.

Despite recent advances in computer technology, the size of the data sets that we were able to record did not afford the kind of resolution that FT-ICR MS users would like to see: the data-processing program that we used, NMR Processing Kernel, had been developed for NMR spectroscopy [55], in which data sets are typically much smaller than in FT-ICR MS, and had been written in 32-bit code. To acquire enough time transients as a function of t_1 to resolve the ions in the "vertical" ω_1 dimension, we had to sacrifice high resolution in the "horizontal" ω_2 dimension. We recorded 2D mass spectra with 2,048 time transients comprising 32,768 data points each, leading to a file size of 256 MB.

The samples we used in this study were well-known peptides, angiotensin I, fragment 1–8 of bradykinin, and substance P. In Fig. 3 we show the 2D FT-ICR MS spectrum of fragment 1–8 of bradykinin with a number of in-source fragments, which are precursor ions in the ICR cell. The 2D mass spectrum features several characteristic lines: the autocorrelation line (circled), which shows the modulation of the relative ICR signal magnitude of the precursor ions with their own cyclotron frequencies, the "horizontal" spectra of fragment ions (horizontal fragment ion spectrum), and the "vertical" spectra of precursor ions (vertical precursor ion spectrum). A short glossary for 2D MS can be found at the end of this article.

We observed fragments similar to those obtained in IRMPD MS/MS spectra, albeit with low intensities because they were excited three times less than their precursor ions. We also observed harmonics of each peak in the vertical dimension because the cyclotron radii of the ions are not modulated sinusoidally, as predicted by Guan and Jones [56]. Horizontally, the resolution of the peaks increases with cyclotron frequency and decreases with *m*/*z* ratio, as expected from Fourier analysis. The resolution in the vertical domain showed the same behavior, i.e., it is inversely proportional to *m* and did not depend on the cyclotron frequency in the horizontal domain. Finally, we observed considerable scintillation noise, which led to vertical stripes in the 2D spectrum at the frequencies of the most intense peaks.

Scintillation noise proved to be a significant problem in 2D FT-ICR MS spectra because spurious peaks can lead to errors in determining fragmentation paths. To remove scintillation noise from 2D mass spectra, we applied an algorithm based on singular value decomposition that was

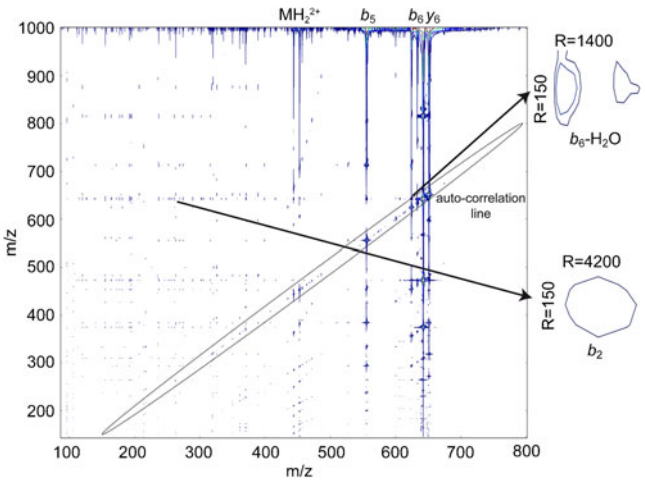

Fig. 3 Two-dimensional FT-ICR MS spectrum of bradykinin using IRMPD fragmentation and Cadzow denoising (30 lines). *Inserts* enlargements of the $b_6 \rightarrow b_6\text{-}H_2O$ and the $b_6 \rightarrow b_2$ peaks. The autocorrelation line is *circled*. (Data published in van Agthoven et al. [59] reprocessed)

developed in 1987 by Cadzow and Wu [57]. This algorithm is based on the postulate that signals can be decomposed into sums of exponentially damped sinusoids, which is the basis of all Fourier analysis, so after a certain number of data points, the next data point can be predicted. No hypothesis about the nature of the noise is required. The data are arranged in a Toeplitz matrix that is decomposed into eigenvectors which can be arranged in decreasing order of their eigenvalues. Depending on an estimate of the noise level, only the eigenvectors with the highest eigenvalues are retained, and the data can be reconstructed. This algorithm can be transposed from NMR spectroscopy, where it has often been successfully applied [58]. It can be applied to each vertical section (parallel to the ω_1 axis) of 2D FT-ICR MS spectra [59].

In Fig. 4 we show how the Cadzow algorithm improves 2D FT-ICR MS spectra. The number of lines corresponds to the number of eigenvectors of the Toeplitz matrix that were retained, the remaining being discarded. We found that as the number of lines decreases, the noise level of the vertical spectra also decreases, thereby decreasing the intensity of the vertical stripes in the 2D FT-ICR MS spectrum and increasing the signal-to-noise ratio. We also found that peaks that had hitherto been lost in the noise could be identified after Cadzow denoising. However, because the origins of scintillation noise in 2D FT-ICR MS have yet to be determined, we could not predict how many of the remaining signals were due to noise, and we had to optimize the number of lines by trial and error.

Figure 5 shows the 2D mass spectrum of substance P obtained with ECD as a fragmentation mode. Like IRMPD, ECD is a gas-free fragmentation mode using an electron beam focused at the center of the ICR cell. ECD is particularly useful for peptides and proteins, because fragmentations are specific to the peptide backbone without affecting posttranslational modifications [60]. Cleavages occur at almost every residue and produce almost exclusively c/z ions. As a result, ECD is very useful to determine the sequence of a peptide or protein and to locate and identify posttranslational modifications.

The 2D ECD mass spectrum of substance P in Fig. 5 [61] is very similar in appearance to the 2D IRMPD mass spectrum in Fig. 4. The autocorrelation line is emphasized by an ellipse. All fragments stemming from a common precursor appear on the same horizontal line. The ECD fragmentation of MH_2^{2+} produced c ions that allowed almost complete sequence coverage of the peptide. The b_{10}^{2+} ion is an in-source fragment and plays the role of a precursor in the ICR cell that is fragmented by ECD. In the vertical ω_1 dimension, the resolution of the peaks decreases with the m/z ratio, as normally observed in FT-ICR mass spectra, and as it also does in the horizontal ω_2 dimension [61].

Future developments in 2D FT-ICR MS

The next steps in the development of 2D FT-ICR MS will involve recording 2D ECD and IRMPD spectra of complex samples such as intact proteins and protein digests. Several problems need to be addressed in order to obtain analytically useful 2D mass spectra. The first issue concerns the harmonics of precursor ion peaks (and, to a lesser extent, of fragment ion peaks) that appear in the vertical dimension. Fragmentation by ECD and IRMPD occurs at the center of the ICR cell, so the modulation of ionic radii resembles a Dirac comb rather than a sinusoid. As a result, harmonics in the vertical dimension are intense. To eliminate these problems, we are considering both pulse sequence parameter

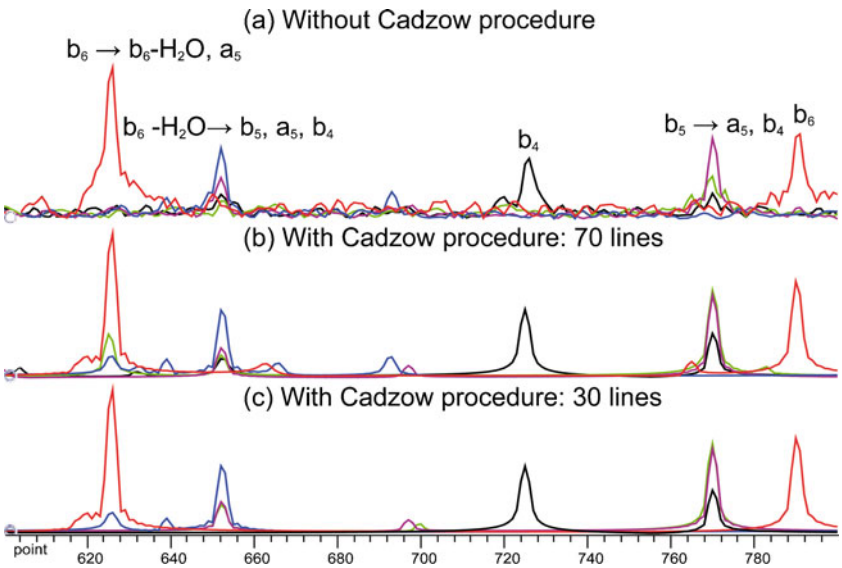

Fig. 4 Spectra of precursor ions taken along the vertical ω_1 dimension of a 2D IRMPD FT-ICR MS spectrum of bradykinin: b_6 (*red*), b_6-H_2O (*blue*), b_5 (*pink*), a_5 (*green*), b_4 (*black*): *a* without the Cadzow algorithm, *b* with the Cadzow algorithm for 70 lines, and *c* with the Cadzow algorithm for 30 lines. (Reproduced with permission from van Agthoven et al. [59])

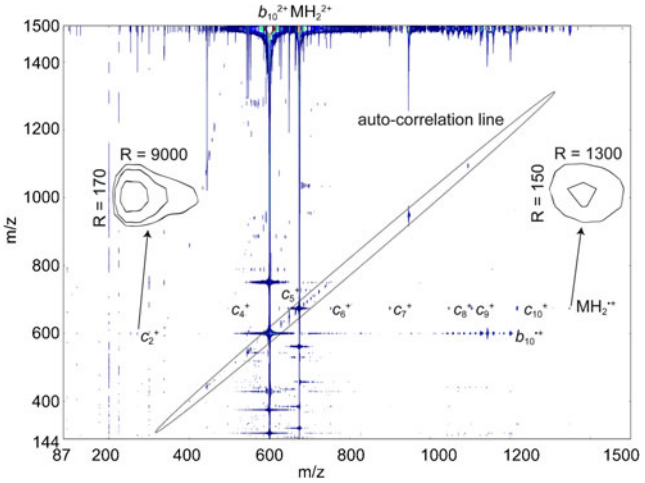

Fig. 5 Two-dimensional ECD FT-ICR mass spectrum of substance P (1 pmol/μL in 50:50 MeOH/H_2O with 0.1% formic acid sprayed at 100 nL/min) with an (*m/z* 87–1,500)×(*m/z* 144–1,500) mass range (1,024 transients each comprising 65,536 data points) using an ECD interval τ_m=0.03 s with a heating current of 1.7 A in the cathode of the electron gun and an electron energy of 1.0 eV. Both axes are labeled in *m/z* ratios. The 2D mass spectrum is presented after Cadzow denoising (seven lines, five iterations, 1,000 order). *Inserts* zoom-ins on the $MH_2^{2+}\rightarrow MH_2^{\bullet+}$ peak and the $b_{10}^{2+}\rightarrow c_2^+$ peak. The autocorrelation line is *circled*

optimization and additional data processing steps, such as investigating frequency correction in the vertical dimension.

Scintillation noise is also an issue that needs to be addressed, as we have seen earlier. The vertical streaks caused by the fluctuation in ion numbers in the ICR cell can mask low-intensity signals and cause mistakes in data interpretation. The Cadzow algorithm has allowed us to denoise 2D mass spectra because it does not presuppose any particular properties of the nature of the noise. However, because we have not yet been able to track down the exact cause of the scintillation noise, the application of the Cadzow algorithm is not fully satisfactory because we have to guess the number of eigenvectors that must be retained and how many may be discarded.

Another problem that is currently being addressed is the size of the data that can be processed. Although the 64-bit 2D FT-ICR MS program that is being developed by the Institut de Génétique et Biologie Moléculaire et Cellulaire and NMRTEC in Illkirch-Graffenstaden (France) can currently handle the 2D mass spectra presented in this article with ease, the size of the data files necessary for high resolution and high accuracy in both dimensions is more than 32 GB. These requirements are much greater than those commonly needed for 2D NMR spectra, although 3D and 4D NMR spectra can also be demanding. Affordable computers do not have enough RAM to compute fast Fourier transforms of such large files. To be able to process them, new file formats and new processing methods need to be developed. In addition, the Cadzow algorithm must be adapted for large files (the 2D mass spectrum shown in Fig. 5 took 1,152 h spread over 48 processors to be denoised). A signal intensity threshold should allow one to avoid lengthy calculations in empty areas of the 2D spectra. Partial singular value decomposition algorithms that are able to handle the very large matrices which are produced in the Cadzow algorithm are also being investigated [62].

The need to record large data sets in order to obtain high-resolution 2D mass spectra leads to protracted experiments and consumes large amounts of sample. Fortunately, there are many partial sampling techniques that can be adapted from 2D NMR spectroscopy to 2D FT-ICR MS in order to reduce the size of the data sets without loss of resolving power. These can lead to shorter experiments and less sample consumption [63]. We are also looking into possibilities offered by alternative pulse sequences, especially by adapting ideas such as the accordion experiment [64] from 2D NMR spectroscopy to 2D FT-ICR MS which may give access to the ion lifetime. We can also obtain high-resolution 2D mass spectra through alternative data processing methods, such as the filter diagonalization method, which shows great promise in 1D FT-ICR MS [14, 65].

Maintaining the coherence of ion packets is very important in 2D FT-ICR experiments. If the ion packets lose their coherence during the pulse sequence, the phase difference between the ion motion and the RF pulse is lost and the overlap between the laser or electron beam and the ions decreases. This causes the fragmentation efficiency to decrease and affects the abundance of fragments and the quality of the data. The geometry of the ICR cell has a great impact on ion packet coherence and can therefore greatly affect the quality of 2D FT-ICR MS spectra. Compensated ICR cells such as those developed by Brustkern et al. [21] and the harmonized cell developed by Nikolaev et al. [23] show great promise in this respect.

Two-dimensional FT-ICR MS shows great potential as an analytical tool. Because ion isolation is not necessary, losses of less abundant ions during transfer from the ion source to the ICR cell are minimized. The fact that the accumulation of time transients benefits all ion species instead of only the ones that have been isolated is an important advantage over MS/MS. Fragmentation modes such as ECD are better adapted for 2D FT-ICR MS than for LC–FT-ICR MS/MS because of the low abundance of fragments and because time transients cannot be accumulated in LC–FT-ICR MS/MS as in 2D FT-ICR MS/MS.

Two-dimensional FT-ICR MS has the potential to provide more information on complex samples than either MS/MS or LC–MS/MS because it reveals the fragmentation patterns of all ion species in a complex sample regardless of their abundance. For abundant samples, bypassing the LC step can be especially advantageous since LC can lead to the loss of entire molecular families. This can be very useful in

many domains such as the analysis of food, soil, petroleum, rainwater, seawater, biomolecules such as intact proteins, protein digests, and other samples of biological origin. As a result, 2D FT-ICR MS could well become an essential part of proteomics, lipidomics, or metabolomics research.

Acknowledgments The FT-ICR mass spectrometer and the proteomics platform used for this study are funded by the European Community (FEDER), the Région Nord–Pas-de-Calais (France), the IBISA network, the CNRS, and Université Lille 1, Sciences et Technologies, and this funding is gratefully acknowledged. Computational resources were provided by the Centre de Ressources Informatiques of Université Lille 1 supported by the CNRS and Université Lille 1. M.v.A. thanks the Région Nord–Pas-de-Calais for postdoctoral funding. The authors gratefully acknowledge funding of this project by the Agence Nationale de la Recherche (grant 2010 FT-ICR 2D). Financial support from the TGE FT-ICR for conducting the research is also gratefully acknowledged. The authors thank the referees for their very careful reading of the manuscript and their suggested corrections.

Glossary

Autocorrelation line	Line with a $y=x$ equation in the 2D mass spectrum, which shows the modulation of the relative ICR signal magnitude of the precursor ions with their own cyclotron frequency. The autocorrelation line is the equivalent of the MS spectrum of the precursor ions.
Encoding pulse	Second pulse (designated P2) of the pulse sequence, which excites or de-excites precursor ions according to their cyclotron frequency and the value of t1.
Encoding sequence	The sequence which encodes the frequencies of the precusor ions prior to fragmention and normally composed of a excitation pulse, an encoding period and an encoding pulse.
Excitation pulse	First pulse (designated P1) of the pulse sequence, which excites all precursor ions equally.
Frequency encoding period	Regularly incremented interval (designated t1) in between the two pulses of the encoding sequence, during which all precursor ions rotate at their cyclotron frequency.
Fragmentation period	Fixed period between the encoding sequence and the observe pulse during which precursor ions are fragmented.
Horizontal fragment ion spectrum	Horizontal cross section of the 2D mass spectrum. The horizontal fragment ion spectrum shows the fragment ion spectrum of the ion species with the m/z ratio where it intersects the autocorrelation line.
Observe pulse	Third pulse (designated P_3) of the pulse sequence, which excites both precursor and fragment ions prior to detection.
Two-dimensional mass spectrum	Two-dimensional spectrum obtained from the time transients acquired using the pulse sequence presented in Fig. 2 with regularly incremented delay t_1, followed by Fourier transformation in two dimensions and conversion of cyclotron frequencies into m/z ratios. By convention 2D mass spectra are plotted with the Fourier transform which corresponds to the transient obtained during time t_2 in the horizontal dimension, whereas the Fourier transform which corresponds to the signal measured with incremental values of t_1 is plotted vertically. This convention respects the usual convention in MS [66].
Vertical precursor ion spectrum	Vertical cross section of the 2D mass spectrum. The vertical precursor ion spectrum shows the precursor ion spectrum of the ion species with the m/z ratio where it intersects the autocorrelation line.

References

1. Comisarow MB, Marshall AG (1974) Chem Phys Lett 25:282
2. Marshall AG (2000) Int J Mass Spectrom 200:331
3. Le Vot C, Afonso C, Beaugrand C, Tabet J-C (2011) Int J Mass Spectrom 306:150
4. Senko MW, Hendrickson CL, Pasa-Tolic L, Marto JA, White FM, Guan S, Marshall AG (1824) Rapid Commun Mass Spectrom 1996:10
5. Belov ME, Nikolaev EN, Anderson GA, Udseth HR, Conrads TP, Veenstra TD, Masselon CD, Gorshkov MV, Smith RD (2001) Anal Chem 73:253
6. Marshall AG, Hendrickson CL, Jackson GS (1998) Mass Spectrom Rev 17:1
7. Kaplan DA, Hartmer R, Speir JP, Stoermer C, Gumerov D, Easterling ML, Brekenfeld A, Kim T, Laukien F, Park MA (2008) Rapid Commun Mass Spectrom 22:271
8. Syka JEP, Marto JA, Bai DL, Horning S, Senko MW, Schwartz JC, Ueberheide B, Garcia B, Busby S, Muratore T, Shabanowitz J, Hunt DF (2004) J Proteome Res 3:621
9. Belov ME, Anderson GA, Angell NH, Shen Y, Tolic N, Udseth HR, Smith RD (2001) Anal Chem 73:5052
10. Hogan JM, Pitteri SJ, Chrisman PA, McLuckey SA (2005) J Proteome Res 4:628
11. Guan S, Li G-Z, Marshall AG (1997) Int J Mass Spectrom Ion Process 167–168:185

12. Boldin IA, Nikolaev EN (2011) Rapid Commun Mass Spectrom 25:122
13. Vining BA, Bossio RE, Marshall AG (1999) Anal Chem 71:460
14. Kozhinov AN, Tsybin YO (2012) Anal Chem 84:2850
15. He F, Hendrickson CL, Marshall AG (2001) Anal Chem 73:647
16. Tolmachev AV, Robinson EW, Wu S, Pasa-Tolic L, Smith RD (2009) Int J Mass Spectrom 287:32
17. Valeja SG, Kaiser NK, Xian F, Hendrickson CL, Rouse JC, Marshall AG (2011) Anal Chem 83:8391
18. Caravatti P, Allemann M (1991) Org Mass Spectrom 26:514
19. Gabrielse G, Haarsma L, Rolston SL (1989) Int J Mass Spectrom Ion Process 88:319
20. Tolmachev AV, Robinson EW, Wu S, Kang H, Lourette NM, Pasa-Tolic L, Smith RD (2008) J Am Soc Mass Spectrom 19:586
21. Brustkern AM, Rempel DL, Gross ML (2008) J Am Soc Mass Spectrom 19:1281
22. Kaiser NK, Savory JJ, McKenna AM, Quinn JP, Hendrickson CL, Marshall AG (2011) Anal Chem 83:6907
23. Nikolaev EN, Boldin IA, Jertz R, Baykut G (2011) J Am Soc Mass Spectrom 22:1125
24. Nikolaev EN, Jertz R, Grigoryev A, Baykut G (2012) Anal Chem 84:2275
25. Nikolaev EN, Gorshkov MV (1985) Int J Mass Spectrom Ion Process 64:115
26. Comisarow MB, Marshall AG (1974) Chem Phys Lett 26:489
27. Marshall AG, Wang TCL, Ricca TL (1985) J Am Chem Soc 107:7893
28. Grosshans PB, Marshall AG (1992) Int J Mass Spectrom Ion Process 115:1
29. Grosshans PB, Chen R, Limbach PA, Marshall AG (1994) Int J Mass Spectrom Ion Process 139:169
30. Gauthier JW, Trautman TR, Jacobson DB (1991) Anal Chim Acta 246:211
31. Marshall AG, Wang TCL, Ricca TL (1984) Chem Phys Lett 105:233
32. Noest AJ, Kort CWF (1983) Comput Chem 7:81
33. Vulpius T, Houriet R (1989) Int J Mass Spectrom Ion Process 88:283
34. Boering KA, Rolfe J, Brauman JI (1992) Rapid Commun Mass Spectrom 6:303
35. Boering KA, Rolfe J, Brauman JI (1992) Int J Mass Spectrom Ion Process 117:357
36. Pfaendler P, Bodenhausen G, Rapin J, Houriet R, Gäumann T (1987) Chem Phys Lett 138:195
37. Pfaendler P, Bodenhausen G, Rapin J, Walser ME, Gäumann T (1988) J Am Chem Soc 110:5625
38. Bensimon M, Zhao G, Gäumann T (1989) Chem Phys Lett 157:97
39. Kumar A, Ernst RR, Wuethrich K (1980) Biochem Biophys Res Commun 95:1
40. Buttrill SE Jr (1973) J Chem Phys 58:656
41. Aue WP, Bartholdi E, Ernst RR (1976) J Chem Phys 64:2229
42. Ross CW III, Guan S, Grosshans PB, Ricca TL, Marshall AG (1993) J Am Chem Soc 115:7854
43. van der Rest G, Marshall AG (2001) Int J Mass Spectrom 210/211, 101
44. Ross CW, Simonsick WJ Jr, Aaserud DJ (2002) Anal Chem 74:4625
45. Reiger SH (1963) Astron J 68:395
46. Morris GA (1992) J Magn Reson 100:316
47. Haebel S, Gäumann T (1995) Int J Mass Spectrom Ion Process 144:139
48. McLafferty FW, Stauffer DB, Loh SY, Williams ER (1987) Anal Chem 59:2212
49. Gao X, Wood TD (1997) Rapid Commun Mass Spectrom 1996:10
50. Panchaud A, Scherl A, Shaffer SA, von Haller PD, Kulasekara HD, Miller SI, Goodlett DR (2009) Anal Chem 81:6481
51. Panchaud A, Jung S, Shaffer SA, Aitchison JD, Goodlett DR (2011) Anal Chem 83:2250
52. Gillet LC, Navarro P, Tate S, Roest H, Selevsek N, Reiter L, Bonner R, Aebersold R (2012) Mol Cell Proteomics
53. Tsybin YO, Witt M, Baykut G, Kjeldsen F, Hakansson P (2003) Rapid Commun Mass Spectrom 17:1759
54. van Agthoven MA, Delsuc M-A, Rolando C (2011) Int J Mass Spectrom 306:196
55. Tramesel D, Catherinot V, Delsuc M-A (2007) J Magn Reson 188:56
56. Guan S, Jones PR (1989) J Chem Phys 91:5291
57. Cadzow JA, Wu M-M (1987) IEE Proc Part F 134:69
58. Brissac C, Malliavin TE, Delsuc MA (1995) J Biomol NMR 6:361
59. van Agthoven MA, Coutouly M-A, Rolando C, Delsuc M-A (2011) Rapid Commun Mass Spectrom 25:1609
60. Cooper HJ, Hakansson K, Marshall AG (2005) Mass Spectrom Rev 24:201
61. van Agthoven MA, Chiron L, Coutouly M-A, Delsuc M-A, Rolando C (2012) Anal Chem 84:5589
62. de Lathauwer L, de Moor B, Vandewalle J (2000) SIAM J Matrix Anal Appl 21:1253
63. Delsuc M-A, Tramesel D (2006) C R Chim 9:364
64. Bodenhausen G, Ernst RR (1982) J Am Chem Soc 104:1304
65. Aizikov K, O'Connor PB (2006) J Am Soc Mass Spectrom 17:836
66. Louris JN, Wright LG, Cooks RG, Schoen AE (1985) Anal Chem 57:2918